Catalysis Today 181 (2012) 33–39

Contents lists available at SciVerse ScienceDirect

Catalysis Today

journal homepage: www.elsevier.com/locate/cattod

Synthesis and characterisation of coiled carbon nanotubes

A. Csató[a], A. Szabó[a], A. Fonseca[b], D. Vuono[b,*], Z. Kónya[c], A. Volodin[d], C. Van Haesendonck[d], L.P. Biro[e], G. Giordano[a], J. B. Nagy[a]

[a] Department of Chemical Engineering and Materials, University of Calabria, via P. Bucci, I-87036 Arcavacata di Rende (CS), Italy
[b] NANOPART S.A., Kapeldreef 60, BE-3001 Leuven, Belgium
[c] Applied and Environmental Chemistry Department, University of Szeged Rerrich Béla tér 1, H-6720 Szeged, Hungary
[d] Laboratory of Solid-State Physics and Magnetism, Katholieke Universiteit Leuven, BE-3001 Leuven, Belgium
[e] Research Institute for Technical Physics and Materials Science, H-1525 Budapest, P.O. Box 49, Hungary

ARTICLE INFO

Article history:
Received 14 March 2011
Received in revised form 4 August 2011
Accepted 17 August 2011
Available online 29 September 2011

Keywords:
Nanocoils
Coils
Nanotubes
CCVD
Coil pitch
Coil diameter

ABSTRACT

Recent results from our group and from literature data are summarized. Emphasis is put on the various supported catalysts that can lead to the formation of helical (or coiled) carbon nanotubes. Detailed analysis of transmission electron microscopy images reveals that not all types of nanotubes – having any type of coil pitch and coil diameter – are equally probable: stability islands can be found in the 3D representation of the number of nanotubes as a function of both coil pitch and coil diameter. In most of the cases the coils are formed by introducing pairs of five-membered and seven-membered rings into the nanotubes containing the basic six-membered rings. Possible applications of the helical carbon nanotubes are discussed.

1. Introduction

Helical or coiled carbon nanotubes were synthesized shortly after the rediscovery of the synthesis of carbon nanotubes by Ijima [1–3]. The coiled carbon nanotubes are formed by introducing pairs of five-membered and seven-membered rings into the basic six-membered rings contained in the nanotubes [4–8]. This formation was already predicted theoretically by Dunlap [9] and Itoh et al. [10,11].

The helical or coiled carbon nanotubes can be formed by catalytic chemical vapour deposition (CCVD) using the decomposition of hydrocarbon on transition metal containing supported catalysts [12]. They can also be obtained by reducing ethyl ether with metallic zinc [13] and they were also observed as by-products in microwave plasma-enhanced CVD [14] or by CCVD pyrolysis of a vapour mixture of $Fe(CO)_5$ and pyridine or toluene [15]. In most of the cases fixed bed reactors were used [4,5,12] for the synthesis of coiled carbon nanotubes, but very recently a fluidised bed was successfully used as well in obtaining them [16]. A triple helix was observed in the product of carbon nanotubes obtained using marine manganese nodule, a naturally occurring mineral [17]. A mixture of helical carbon nanotubes, worm-like carbon nanotubes and nanocoils could be obtained at a low temperature of 450 °C in high yield using Fe deposited on a ceramic plate [18]. FeMo supported on MgO prepared by a combustion method using citric acid as foaming and combustion additive, also leads to the formation of coiled carbon nanotubes [19]. Finally, polyethylene pyrolysis was successful in the formation of coiled carbon nanotubes in presence of ferrocene [20].

In the present paper, we describe the synthesis and characterisation of coiled carbon nanotubes and their possible applications will be reviewed, too.

2. Material and methods

2.1. Synthesis of coiled carbon nanotubes

The synthesis was carried out by catalytic chemical vapour deposition (CCVD) of carbon issued from the catalytic decomposition of acetylene on supported metal catalysts. The catalyst preparation included the impregnation procedure, the ion-adsorption precipitation (IAP) and the sol–gel (SG) process. The impregnation is made on zeolite and Al_2O_3 supports. The ion-adsorption is used for silica gel and $CaCO_3$, while the sol–gel process is applied to prepare silica.

* Corresponding author. Tel.: +32 0984496669; fax: +32 0984496655.
E-mail address: danivuono@gmail.com (D. Vuono).

0920-5861/$ – see front matter © 2011 Elsevier B.V. All rights reserved.
doi:10.1016/j.cattod.2011.08.036

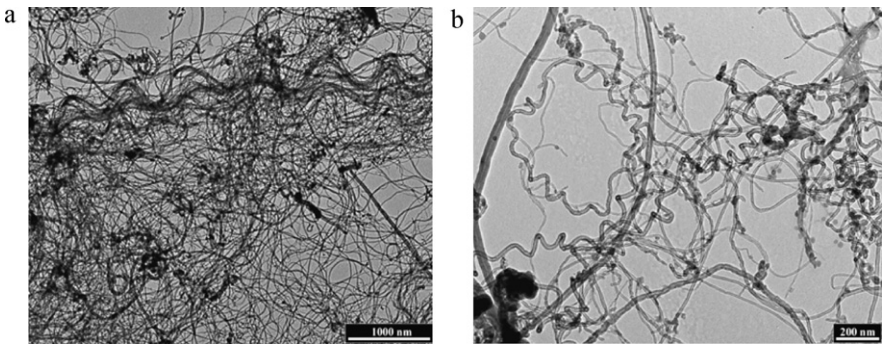

Fig. 1. TEM images of CNTs produced on Al_2O_3 and $CaCO_3$ supported catalysts: (a) Co-Fe/Al_2O_3; (b) Co-Fe/$CaCO_3$ [12].

Since the pH values have a definite influence on the yield of coiled carbon nanotubes, a 8–9 value was maintained in all preparations using ammonia solution [21].

The precursor salts, the supports, the hydrocarbons and the carrier gas are summarized in Table 1.

The synthesis was carried out in a quartz reactor (length: 100 cm; diameter: 5 cm). 1 g of catalyst was placed in a quartz boat forming a shallow bed. The boat was placed into the horizontal reactor at 700 °C and purged with N_2 during 10 min. Acetylene was introduced and the catalytic decomposition of the carbon source started under the following conditions: carrier gas flux of N_2: 300 ml/min; flux of C_2H_2: 30 ml/min; reaction time: 30 min. At the end of the nanotube formation the quartz reactor was taken out of the oven, cooled to room temperature under N_2 flux, and finally the product was weighed. The amount of deposited carbon was computed from:

$$\text{Carbon deposit (wt\%)} = \frac{(m_{\text{product}} - m_{\text{catalyst}})}{m_{\text{catalyst}}} \times 100.$$

The weight of the catalyst (m_{catalyst}) is that of the dried form.

2.2. Characterisation techniques

The low-resolution transmission electron microscopy (TEM) pictures were taken on a Philips CM10 transmission electron microscope using 100 V accelerating voltage. Sample preparation relied on the classical method. About 10 mg of CNT were suspended in 3 ml ethanol and the suspension was then deposited on a carbonated Cu–Rh grid. Several pictures were analysed using the Soft Imaging Viewer software [22].

The % of coiled carbon nanotubes was measured on various TEM pictures containing ca. 400–500 nanotubes.

The distribution of outer diameter of the carbon nanotubes was measured on ca. 500 nanotubes taken in various TEM pictures. The coil diameter and pitch values were obtained from TEM images evaluating in a correlated way, i.e. a 3D plot was used to plot the number of coils exhibiting a certain pair of coil diameter and pitch value [23].

Table 1
Materials.

Catalyst preparation	$Co(CH_3COO)_2{\cdot}4H_2O$ (Aldrich); $Fe(NO_3)_3{\cdot}6H_2O$ (Aldrich); $Co(NO_3)_2{\cdot}6H_2O$ (Vel); $Pr(NO_3)_3{\cdot}9H_2O$ (Aldrich); NaY-FAU zeolite; SiO_2 – 15–40 μm, 30–50 μm, 45–70 μm (Merck, Aldrich); Al_2O_3 (Aldrich); $CaCO_3$ (Aldrich); Tetraethyl-orthosilicate (Acros); NH_3 (Vel); HF (Vel)
NTs synthesis	C_2H_2 (Air Liquide); N_2 (Air Liquide)
Microscopy	Ethanol (Fluka); Aceton (Vel)

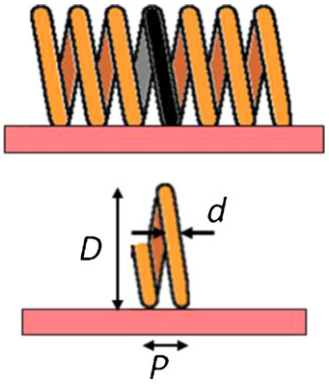

Fig. 2. Schematic illustration of our definition of coil diameter (D), coil pitch (P) and nanotube outer diameter (d) for a coiled carbon nanotube [12].

3. Results and discussion

In Table 2 we present the TEM results obtained on various catalysts.

The Al_2O_3 supported Co-Fe catalyst demonstrated high activity in the formation of carbon nanotubes. The obtained carbon deposit is high and the TEM micrographs and thermal analysis suggest insignificant formation of amorphous carbon. In some cases the nanotubes form slightly waved fibre like structures, probably because of their length. Still the formation of helical or coiled CNTs using this support material was insignificant (Fig. 1(a)).

Irregularly coiled and waved carbon nanotubes were produced on the Co-Fe/$CaCO_3$ (Fig. 1(b)). The average coil diameter was in the range of 50–100 nm in this case.

All zeolite supported catalysts demonstrated less activity in the formation of CNTs than the other ones.

SiO_2 supported catalysts revealed the formation of coiled CNTs with more regular shape. They presented a telephone wire-like, spring-like or sinusoid-like morphology with different coil diameters and pitches. The coil diameter D, the coil pitch P and the nanotube outer diameter are defined in Fig. 2.

Table 2
Quality[a] of the NTs produced on various catalysts, according to TEM observation [12].

Support	Al_2O_3	$CaCO_3$	NaY-FAU		
Metal(s)	Co-Fe	Co-Fe	Fe	Co-Fe	Co
Wt% metal(s)	3.5–1.5	3.5–1.5	5.0	2.5–2.5	5.0
Coiled NTs	+	+	+	+	+
Straight NTs	++++	++++	++	++	++
C. Deposit (wt%)	70	20	30	20	20

[a] The quality of the carbon material was defined as follows: ++++ very high density; +++ high density; ++ medium density; + low density.

Table 3
Quality of the NTs synthesized on Fe, Co and Pr supported on SiO_2 produced by the IAP method.

Co (wt%)	5	10	2.5	1	4		2.5	1	4	5	2.5	7.5
Fe (wt%)			2.5	4	1	5						
Pr (wt%)							2.5	4	1	5	7.5	2.5
CD[a] (wt%)	58	38	42	41	42	41	63	53	57	50	10	63
% Coiled NT	5	5	<5	-	<5	-	15	16	10	10	<5	5

[a] CD: carbon deposit

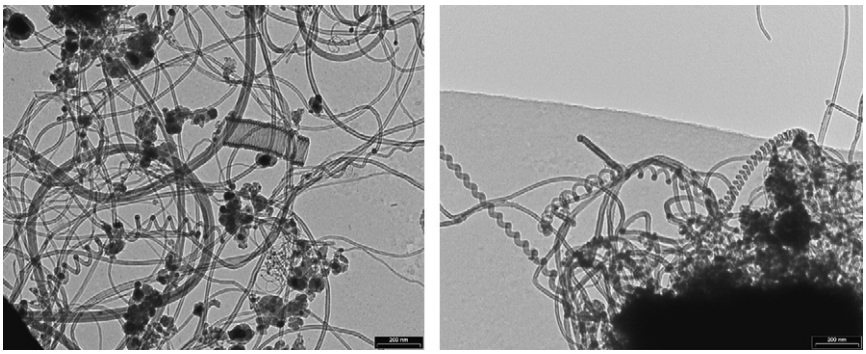

Fig. 3. TEM images of CNTs synthesized on 2.5%Co-2.5%Pr/SiO_2.

A series of SiO_2 supported catalysts were recently prepared using the IAP method and the results are summarized in Table 3.

The percentage of coiled CNTs is calculated from all the counted tubes (ca. 400–500). The Co-Pr bimetallic and the Co containing monometallic catalysts turned out to be the most promising as far as the coiled CNT formation is concerned. The Co containing catalysts resulted in higher CNT formation and less deposit of amorphous carbon. Although the catalysts containing Co-Pr lead to the formation of less carbon nanotubes and more amorphous carbon, the proportion of coiled CNTs compared to the straight ones is found to be higher. A series of synthesis reactions was performed using Co/SiO_2 catalyst prepared by ion-adsorption-precipitation technique (Fig. 3). These catalysts also resulted in a high yield of coiled carbon nanotubes.

In Fig. 4 we present TEM images of the products obtained on the Co/SiO_2 catalysts. As it can be seen, the concentration of helical or coiled carbon nanotubes is sufficiently high in both cases. The coils present various morphologies and diameters, but at the same time they demonstrate a certain regularity. The diameter of the "dense" coiled tubes varies between 100 and 150 nm, while the pitch varies between 10 and 15 nm. In most of the cases the coil diameter is in the range of 30–150 nm, rarely the diameter exceeds 300 nm. Generally, the coil pitch is in the 50–200 nm range. Their length varies between 2 and 5 μm. Occasionally, a change of the pitch or coil diameter can be observed (see white arrow in Fig. 4(a)). There exist several hypotheses trying to explain why this phenomenon occurs, but a reliable explanation is still missing.

Co/SiO_2 catalysts were also prepared by a sol–gel (SG) process. The metal loading varied from 1 to 11.7%. The best catalyst turned out to be the one with the 11.7% metal loading, although the other catalysts with a metal concentration higher than 5% also showed high efficacy in the formation of coiled CNTs. In Fig. 5 we present TEM images of the coils obtained on these catalysts.

The coil pitch of the coiled carbon nanotubes prepared by the SG process is smaller and more regular than that of the coiled tubes synthesized on catalysts prepared by the IAP method, and is in the range of 30–100 nm. As it can be seen from the TEM images, the helices have the morphology of elongated telephone wire and dense spring, while the coils obtained on IAP catalysts are more sinusoid and "S" shaped with a larger pitch. The coil diameter also varies in the range of 30–100 nm. The length is 2–5 μm.

The $Co\text{-}Pr/SiO_2$ catalyst demonstrated high activity in the formation of regular coils. Therefore, a series of samples was recently prepared using different Co-Pr loading (see Fig. 6). According to the experimental results, the best metal proportions for this catalyst seem to be the 1 wt%Co-4 wt%Pr catalyst. However, in the samples produced using this catalyst a significant amount of amorphous carbon can be observed, and the number of coiled CNTs compared to the straight ones is higher. Since by purification and oxidation the amorphous carbon is removed quite easily, a sample with high

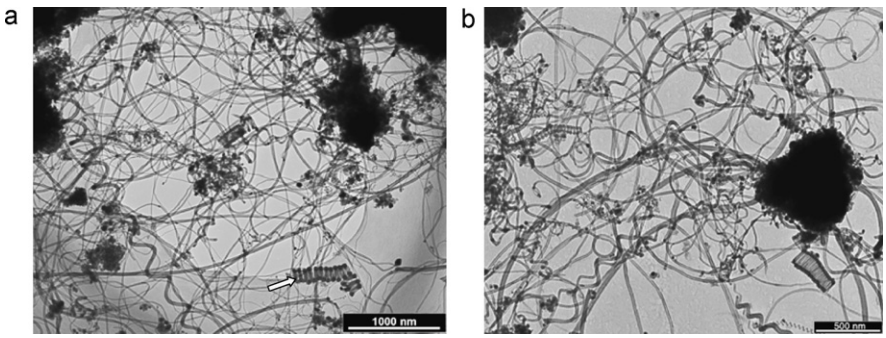

Fig. 4. TEM images of CNTs obtained on Co/SiO_2 catalyst prepared by the IAP method: (a) 5 wt% of Co and (b) 10 wt% Co. The presence of a "dense" coiled tube is indicated by the white arrow [12,28,41].

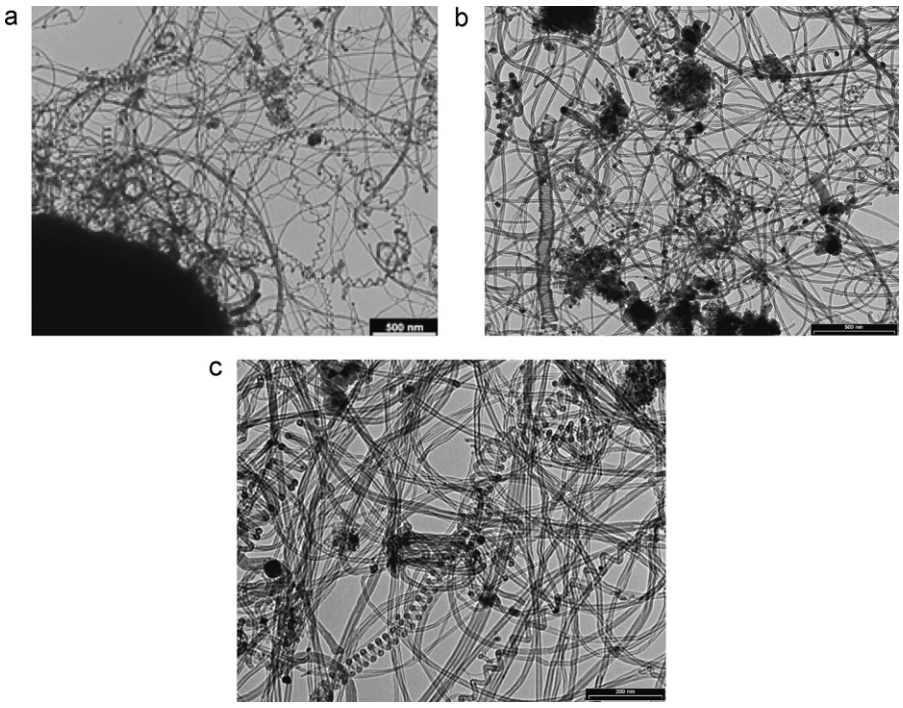

Fig. 5. TEM images of coils synthesized on Co/SiO_2 catalysts prepared by the sol–gel process: (a) 11.7 wt% Co [12]; (b) 8.8 wt% Co; (c) 5.8 wt% Co.

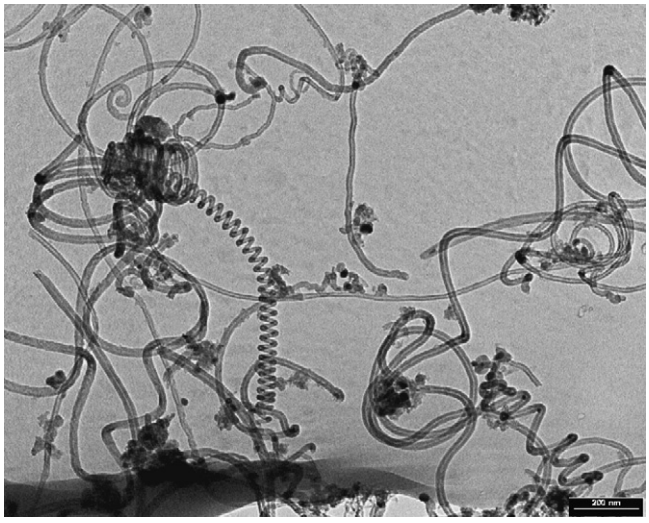

Fig. 6. CNTs on 2.5 wt% Co-2.5 wt% Pr/SiO_2 catalyst prepared by the IAP method.

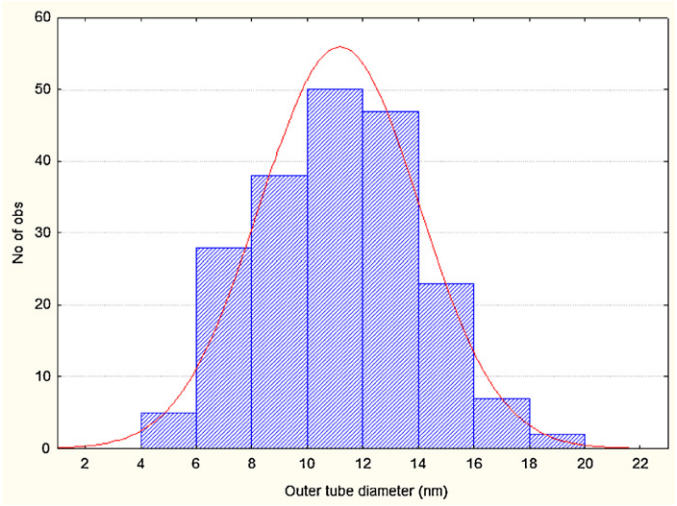

Fig. 7. Distribution of the outer diameter of the CNTs synthesized on the 1%Co-4%Pr/SiO_2 catalyst.

content of coiled tubes could be obtained. The distribution of the outer diameter of the helical CNTs synthesized on the 1% Co-4% Pr supported on SiO_2 is presented in Fig. 7.

The diameters of helical nanotubes produced on these catalysts vary from 10 to 15 nm, the coil pitches are between 30 and 110 nm, and the coil diameters range from 35 to 85 nm. Generally, they are more sinusoidal or S-like shaped and dense coils (Fig. 8(e)) can be observed occasionally. Compared to the coiled CNTs produced on the Co/SiO_2 catalysts, these tubes are thinner and have smaller pitches and coil diameters. The tubes are also shorter, seldom the change of the coil pitch and coil diameter was observed. Besides the regularly coiled tubes numerous wavy CNTs with slight curvatures were found.

The coil pitch of carbon nanotubes synthesized on catalysts obtained by the ion-adsorption precipitation (IAP) method is in the 30–160 nm range, while that of the nanotubes prepared by the sol–gel (SG) method is smaller, i.e. in the range of 30–100 nm. In the first case larger values up to 160 nm could be found in great number which is their characteristic. Occasionally, the pitch may go up to 500 nm. In that case the coiled nanotubes had an elongated 'S' shape, while the coil diameter did not necessarily become larger.

The coil diameter generally varied between 30 and 150 nm for both types of coiled nanotubes but the most frequent values were found in the range of 20–80 nm. The diameter of coils formed on IAP catalysts may exceed 100 nm, even go up to 500 nm, while the coils obtained on SG catalysts had a smaller coil diameter. In this case helices with a diameter smaller than 30 nm were observed in a non-negligible amount.

The diameter of the carbon nanotubes themselves varied only in the range of 10–30 nm. However, most of the nanotube diameters were found in the range of 10–25 nm. Nanotubes having a diameter smaller than 10 nm could also be found occasionally.

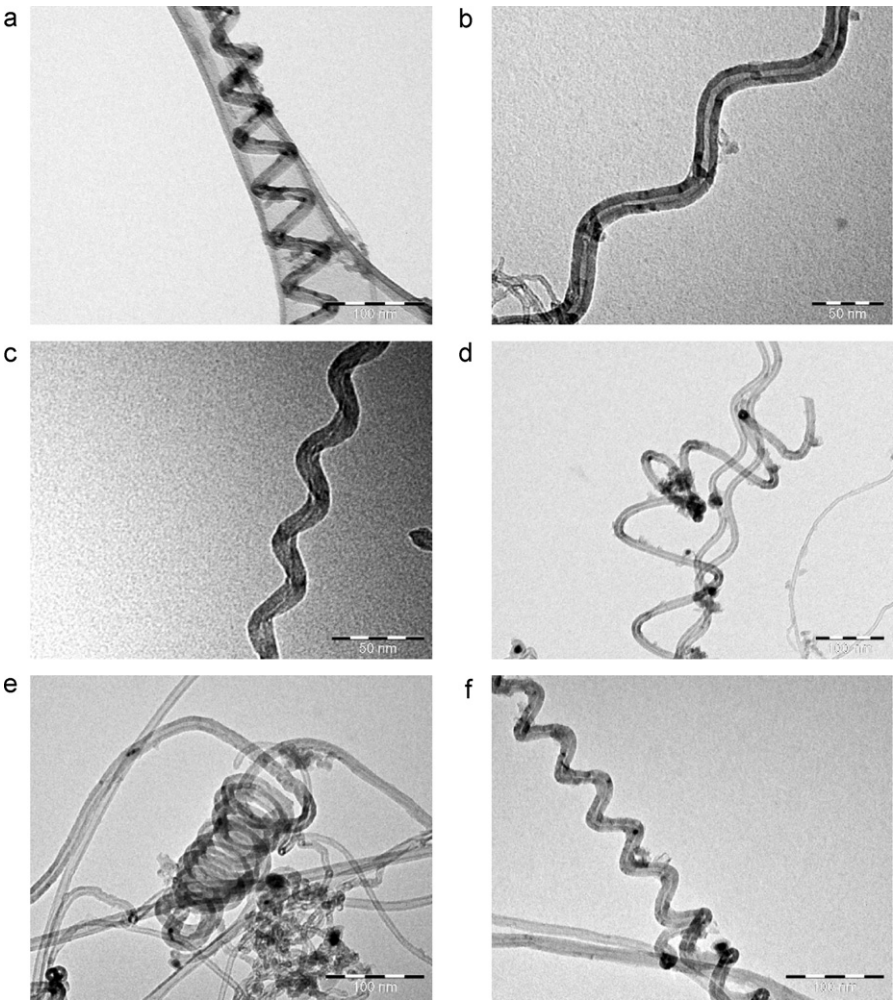

Fig. 8. Helical CNTs with different coil diameter and coil pitch synthesized on Co-Pr/SiO_2 catalysts with different metal loadings: (a) 2.5%Co-5%Pr; (b) and (c) 7.5%Co-2.5%Pr; (d) 5%Co-5%Pr; (e) and (f) 1%Co-4%Pr.

Moreover, it was observed that the diameter of the nanotubes was smaller for the small coil pitch values, for which it varied between 5 and 15 nm. This value increased further to 20–25 nm for larger pitch values. We note that in general a small diameter of the nanotubes corresponded to small pitch values. However, exceptions were observed. Some nanotubes with 30 nm diameter could be observed for coil pitches smaller than 100 nm. For higher pitch values around 150 nm a nanotube diameter of 35–40 nm occurred more frequently.

The distribution of the diameters of the nanotubes was similar to that observed for the coil pitch variation. Smaller coil diameter corresponded to smaller nanotube diameter (in the range of 5–10 nm). The nanotube diameter increased up to a coil diameter of 150 nm. Starting from this value of the coil diameter, the nanotube diameter decreased and mainly small nanotube diameters were observed.

The analysis of the coil diameter, its pitch and the diameter of the carbon nanotubes leads to interesting conclusions.

In Fig. 9 a three-dimensional illustration is presented for the correlation between the number of coiled carbon nanotubes as a function of coil pitch and coil diameter. We clearly are able to identify regions with a higher number of coils when compared to other regions. The regions with a higher number of coils are referred to as "stability islands".

It is obvious that not all helical carbon nanotubes are formed with the same probability. Indeed, two stability islands can be easily identified in Fig. 9.

Table 4
The most frequently encountered coil pitch and coil diameter for the first (1) and the second (2) stability island [12,23].

Type	Coil pitch P (nm)	Coil diameter D (nm)	NT diameter d (nm)	P/R	Amount (%)
1.1	50	30	12	5.6	5
1.2	60	50	13	3.2	5
1.3	70	50	15	4.0	4
2.1	30	30	10	3.0	3
2.2	30	50	12	1.5	2.5
2.3	40	30	12	4.5	2.5
2.4	50	50	15	2.8	2.5

The coil curvature (ζ) is defined as

$$\zeta = \frac{(R^2 + (P/2\pi)2)}{R},$$

with $R = (D - d)/2$. R is the coil radius, D is the coil diameter, d is the diameter of the coiled carbon nanotube and P is the coil pitch. The most frequently found coil curvature is around 25 nm.

The first stability island is in the region of 50–70 nm coil pitch and 20–60 nm coil diameter (Fig. 9). The second stability island is in the 30–50 nm range for both coil pitch and coil diameter (Fig. 9). In Table 4 we present the values of P, D, d, the ratio P/R and the relative

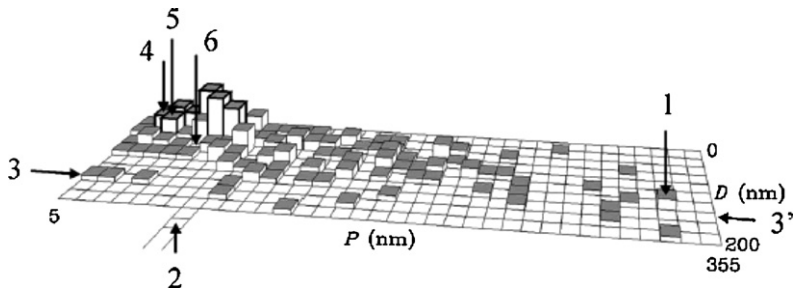

Fig. 9. 3D representation of the distribution of coiled CNTs as a function of coil pitch (P) and coil diameter (D). The two stability islands mentioned in the text are marked by bold lines. Labelled arrows indicate the position of coils that are mentioned in the text: 1 and 2 [23], 3 [24], 4 [25], 5 and 6 [26,27].

% for both stability islands. The new results confirm this previously found correlation.

Several research groups have examined the coiled nanotubes using HRTEM. Bernaerts et al. [24] and Zhang and Zhang [25] have described coils composed of straight segments belonging to the minor components 1, 2 and 3 in Fig. 9. The coil numbered 4 has a coil diameter $D = 52$ nm and its coil pitch $P = 35$ nm is situated at the border of the second stability island. This coil shows a continuous curvature [26]. Biro et al. [27] have found both types of coil in their samples. The coil composed of straight segments is No. 5 in Fig. 9 and it is the first stability island. The coil with a continuous curvature (No. 6 in Fig. 9) is at the border of the second stability island. The properties of the coiled nanotubes that compose the two stability islands are quite close – similar coil pitch and coil diameter – or the coil pitch is smaller than the coil diameter. As a conclusion, it is not possible at present, to tell which structural solution can be expected in the coiled nanotubes.

4. Possible applications of coiled carbon nanotubes

The coiled carbon nanotubes have great potential for applications in nanocomposites, nanoelectronic devices and nanoelectromechanical systems (NEMS). The helix-shaped windings of a suspended helical carbon nanotube reveal characteristic mechanical resonances that are determined by the elastic modulus, mass, shape and dimensions [28–30]. The suspended windings could be resonantly excited in situ at their fundamental frequency by an ultrasonic transducer connected to the substrate [29]. When the tip of the atomic force microscope (AFM) is positioned above a winding, the cantilever is unable to follow its fast oscillations. Nevertheless, an oscillation–amplitude dependent signal is generated due to the nonlinear force-to-distance dependence. The helix-shaped CNTs can be used as high-frequency mechanical resonators.

In another experiment, narrow (around 150 nm) gold electrodes were deposited on the nanotube surface [31]. When the nanotube windings were excited either electrically or acoustically, the contacts between the gold and the coiled nanotube turned out to be extremely sensitive to vibrations, to the point being able to detect fundamental resonances in the range of 100–400 MHz. This way, the coiled carbon nanotubes could be used as mechanical resonant sensors, which are well suited for measuring small forces and masses in the femtogram range [31].

In an experiment carried out by Chen et al. [32] an individual coiled carbon nanotube was clamped between two AFM cantilevers and loaded with tension to a maximum relative elongation of 42%. The results indicated elastic spring behaviour of the coil with a spring constant K of 0.12 N/m in the low-strain regime.

Coiled carbon nanotubes may have more interesting applications in various fields when compared to their straight counterparts. The conduction of electricity through coiled nanotubes can possibly be used for the construction of electromagnetic nanotransformers or nanoswitches. Due to their unique 3D structure, coiled carbon nanotubes may serve in the future as mechanical components that include resonating elements, nanosprings, high performances electromagnetic absorbers and nanoactivators.

The nanocomposites formed by coiled carbon nanotubes and a polymer matrix can be expected to exhibit peculiar mechanical properties. A high Young modulus around 0.7 TPa was determined by Volodin et al. [30]. Moreover, considering the problems related to the interfacial bonding between straight nanotubes and the matrix, i.e. the outermost layer of multiwall nanotubes always tends to pull out from the matrix, the coiled carbon nanotubes as nanofillers may provide an efficient way to improve the interfacial bonding behaviour and the fracture mechanism of nanocomposites [33]. Very recently, mechanical properties of SWNTs-epoxy nanocomposities and coiled nanotube-epoxy nanocomposites were compared and the different reinforcing ability and fracture mechanism were discussed [31]. Vicker's hardness measurements showed that the coiled carbon nanotubes were superior to SWNTs in hardening the matrix by about three times. The fractural strength of the coil-epoxy nanocomposites was higher than for the SWNTs-epoxy composites. Fracture surfaces revealed that the SWNTs-epoxy nanocomposites were broken in a ductile manner with poor adhesion between the SWNTs and the epoxy, while coil-epoxy composites were fractured in a brittle manner with good mechanical interlocking between coils and the epoxy matrix [34,35].

Based on theoretical studies regularly coiled carbon nanotubes are predicted to exhibit exceptional mechanical, electrical and magnetic properties due to the combination of their peculiar helical morphology and the functional properties of the nanotubes [33]. In addition to metallic and semi-conducting behaviour, the coiled nanotubes can even show semi-metallic characteristics due to a high density of states at the Fermi level [36,37]. Such a sharp peak at the Fermi level may result in interesting properties, including superconducting properties [37].

Hydrogen storage in coiled carbon nanotubes was considered from a theoretical point of view [38]. The binding energy values between the hydrogen molecule and the coiled carbon nanotube – considering either a pentagon, a hexagon or a heptagon – are higher (by 50–80%) than the corresponding values in straight carbon nanotubes having similar diameters. The computed storage capacity is 6.8 wt%. Unfortunately, coiled single wall nanotubes are presently still very rare objects [39,40].

5. Conclusions

The CCVD method is very efficient in obtaining coiled carbon nanotubes, although their relative amount is still quite small when compared to the total amount of CNTs that is produced. The coil pitch and coil diameter are governed by "stability islands", where

specific sizes of coiled nanotubes occur preferentially. Due to their special configuration coiled carbon nanotubes have great potential for being used in composite materials. In addition to nanocomposite reinforcement, the coiled CNTs may also be used as mechanical or as electrical sensors. The great challenge remains, however, to synthesize them in sufficiently large quantities.

References

[1] S. Iijima, Nature 354 (1991) 56–58.
[2] L.B. Raduchkevich, V.M. Luk'yanovitch, Chem. Phys. Rev. (URSS) 26 (1952) 88–95.
[3] A. Oberlin, M. Endo, T. Koyama, J. Cryst. Growth 32 (1976) 335–349.
[4] S. Amelinckx, X.B. Zhang, D. Bernaerts, X.F. Zhang, V. Ivanov, J.B. Nagy, Science 265 (1994) 635–639.
[5] X.B. Zhang, X.F. Zhang, D. Bernaerts, G. Van Tendeloo, S. Amelinckx, J. Van Landuyt, V. Ivanov, J.B. Nagy, Ph. Lambin, A.A. Lucas, Europhys. Lett. 27 (1994) 141–146.
[6] L.P. Biro, R. Echlich, Z. Osvath, A. Koos, Z.E. Horvath, J.B. Nagy, J. Gyulai, Mater. Sci. Eng. C19 (2002) 3–7.
[7] L.P. Biró, G.I. Márk, A.A. Koós, J.B. Nagy, Ph. Lambin, Phys. Rev. B 66 (2002) 165405-1–165405-6.
[8] Ph. Lambin, G.I. Márk, L.P. Biró, Phys. Rev. B 67 (2003) 205413-1–205413-9.
[9] B.I. Dunlap, Phys. Rev. B 49 (1994) 5643–5651.
[10] S. Itoh, S. Ihara, J. Kitakami, Phys. Rev. B 47 (1993) 1703–1704.
[11] S. Itoh, S. Ihara, Phys. Rev. B 48 (1993) 8323–8328.
[12] A. Szabo, A. Fonseca, L.P. Biro, Z. Konya, I. Kiricsi, A. Volodin, C. Van Haesendonck, J.B. Nagy, Nanopages 1 (2006) 263–293.
[13] T. Luo, J. Liu, L. Chen, S. Zhang, Y. Qian, Carbon 43 (2005) 755–759.
[14] X. Wang, Z. Hu, Q. Wu, X. Chen, Y. Chen, Thin Solid Films 390 (2001) 130–133.
[15] H.Q. Hou, Z. Jun, F. Weller, A. Greiner, Chem. Mater. 15 (2003) 3170–3175.
[16] J. Liu, A.T. Harris, J. Nanopart. Res. 12 (2010) 645–653.
[17] J. Cheng, X. Zhang, J. Tu, X. Tao, Y. Ye, F. Liu, Mater. Chem. Phys. 95 (2006) 12–15.
[18] X. Qi, W. Zhang, Y. Deng, C. Au, Y. Du, Carbon 48 (2010) 365–376.
[19] T. Somanathan, A. Pandurangan, New Carbon Mater. 25 (2010) 175–180.
[20] Q. Kong, J. Zhang, Polym. Degrad. Stab. 92 (2007) 2005–2010.
[21] K. Hernadi, L. Thien-Nga, L. Forro, J. Phys. Chem. 105 (2001) 12464–12468.
[22] Olympus Soft Imaging Viewer, Olympus Soft Imaging Solutions GmbH, copyright 2003–2009.
[23] A. Szabó, A. Fonseca, J.B. Nagy, Ph. Lambin, L.P. Biró, Carbon 43 (2005) 1628–1633.
[24] D. Bernaerts, X.B. Zhang, X.F. Zhang, S. Amelinckx, G. Van Tendeloo, J. Van Landuyt, V. Ivanov, J.B. Nagy, Philos. Mag. A 71 (1995) 605–630.
[25] X.F. Zhang, Z. Zhang, Phys. Rev. B 52 (1995) 5313–5317.
[26] A.V. Saveliev, W. Mercham-Merchan, L.A. Kennedy, Combust. Flame 135 (2003) 27–33.
[27] L.P. Biro, G.I. Mark, A.A. Koos, Z.E. Horvath, A. Szabo, A. Fonseca, J.B. Nagy, J.-F. Colomer, Ph. Lambin, V. Meunier, C. Charlier, O.N. Bedoya-Martinez, E. Hernandez, Fullerenes Nanotubes Carbon Nanostruct. 13 (2005) 523–533.
[28] A. Szabo, A. Fonseca, A. Volodin, C. Van Haesendonck, L.P. Biro, J.B. Nagy, AIP Proc. 723 (2004) 40–44.
[29] A. Volodin, C. Van Haesendonck, R. Tarkiainen, M. Ahlskog, A. Fonseca, J.B. Nagy, Appl. Phys. A 72 (2001) S75–S78.
[30] A. Volodin, M. Ahlskog, E. Seynaeve, C. Van Haesendonck, A. Fonseca, J.B. Nagy, Phys. Rev. Lett. 84 (2000) 3342–3345.
[31] A. Volodin, D. Buntinx, M. Ahlskog, A. Fonseca, J.B. Nagy, C. Van Haesendonck, Nano Lett. 4 (2004) 1775–1779.
[32] X. Chen, S. Zhang, D.A. Dikin, W. Ding, R.S. Ruoff, Nano Lett. 3 (2003) 1299–1304.
[33] K.T. Lau, M. Lu, D. Hui, Composites: Part B 37 (2006) 437–448.
[34] K.T. Lau, M. Lu, K. Liao, Composites: Part A 37 (2006) 1837–1840.
[35] X.-F. Li, K.-T. Lau, Y.-Sh. Yin, Compos. Sci. Technol. 68 (2008) 2876–2881.
[36] K. Akagi, R. Tamura, M. Tsukuda, S. Itoh, S. Ihara, Phys. Rev. B 53 (1996) 2114–2120.
[37] K. Akagi, R. Tamura, M. Tsukuda, Phys. Rev. Lett. 74 (1995) 2307–2310.
[38] V. Gayathri, N.R. Devi, R. Geetha, Int. J. Hydrogen Energy 35 (2010) 1313–1320.
[39] L.P. Biro, S.D. Lasarescu, P.A. Thiry, A. Fonseca, J.B. Nagy, A.A. Lucas, Ph. Lambin, Europhys. Lett. 50 (2000) 494–500.
[40] L.P. Biro, S. Lazarescu, Ph. Lambin, P.A. Thiry, A. Fonseca, J.B. Nagy, A.A. Lucas, Phys. Rev. B 56 (1997) 12490–12498.
[41] C. Van Haesendonck, L.P. Biro, J.F. Colomer, Fullerenes Nanotubes Carbon Nanostruct. 13 (2005) 139–146.